iScience, Volume *25*

Supplemental information

Deconvolution of the hematopoietic stem cell microenvironment reveals a high degree of specialization and conservation

Jin Ye, Isabel A. Calvo, Itziar Cenzano, Amaia Vilas, Xabier Martinez-de-Morentin, Miren Lasaga, Diego Alignani, Bruno Paiva, Ana C. Viñado, Patxi San Martin-Uriz, Juan P. Romero, Delia Quilez Agreda, Marta Miñana Barrios, Ignacio Sancho-González, Gabriele Todisco, Luca Malcovati, Nuria Planell, Borja Saez, Jesper N. Tegner, Felipe Prosper, and David Gomez-Cabrero

Supplementary Figures

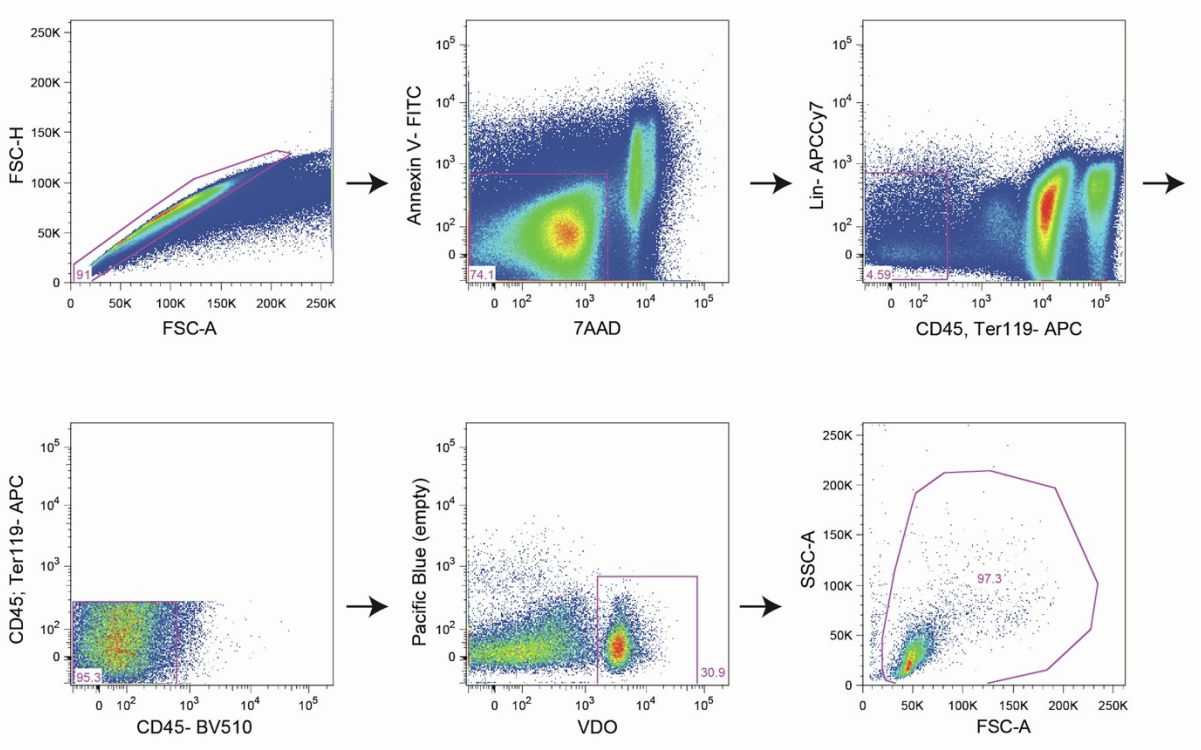

Figure S1. Cell sorting strategy for in-house dataset, related to Figure 1. Cell sorting strategy for isolation of mouse BM microenvironment cells (Lived niche cells: Annexin V^- 7- AAD^- Lin^- $CD45^-$ $Ter119^-$ VDO^+).

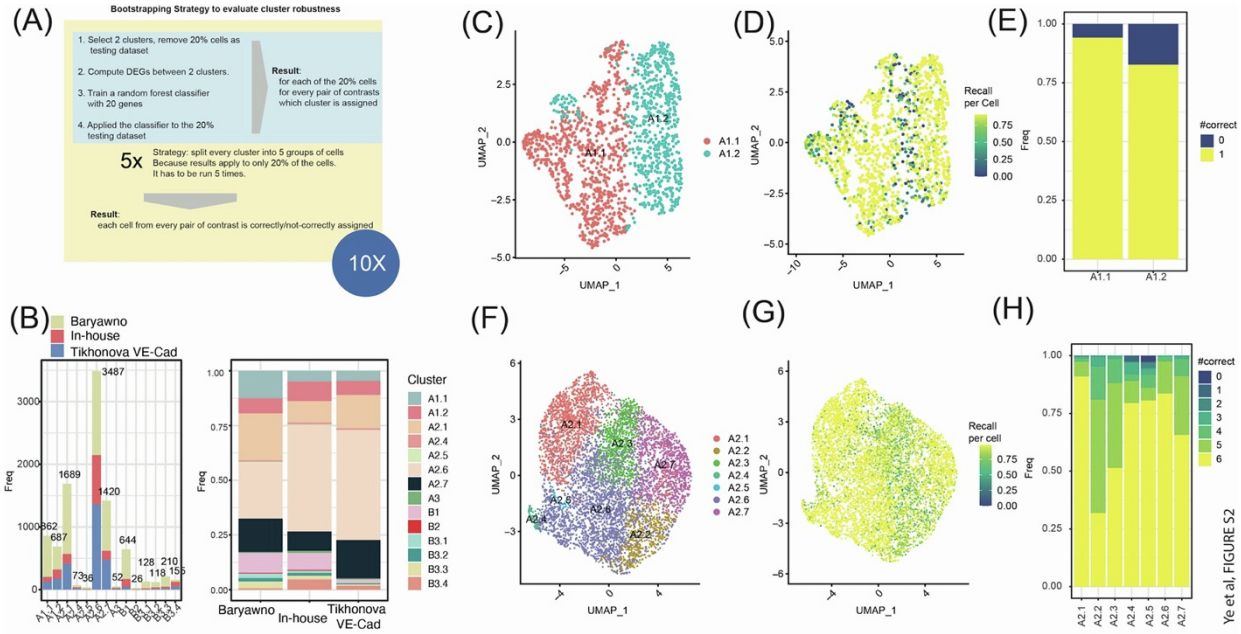

Figure S2. Additional information on the clustering analysis, related to Figure 2. **(A)** Description of the bootstrapping strategy for evaluation cluster robustness (see also Methods). **(B)** Left: representation of the number of cells for each cluster and contribution of each dataset to the final endothelial clusters. Right: proportions of subclusters in each data-set. **(C-E)** Illustration of the sub-clustering, recall per cell and summary of recall per cells for every cluster respectively for the analysis of cluster A1. **(F-H)** Demonstration of the same analysis for cluster A2.

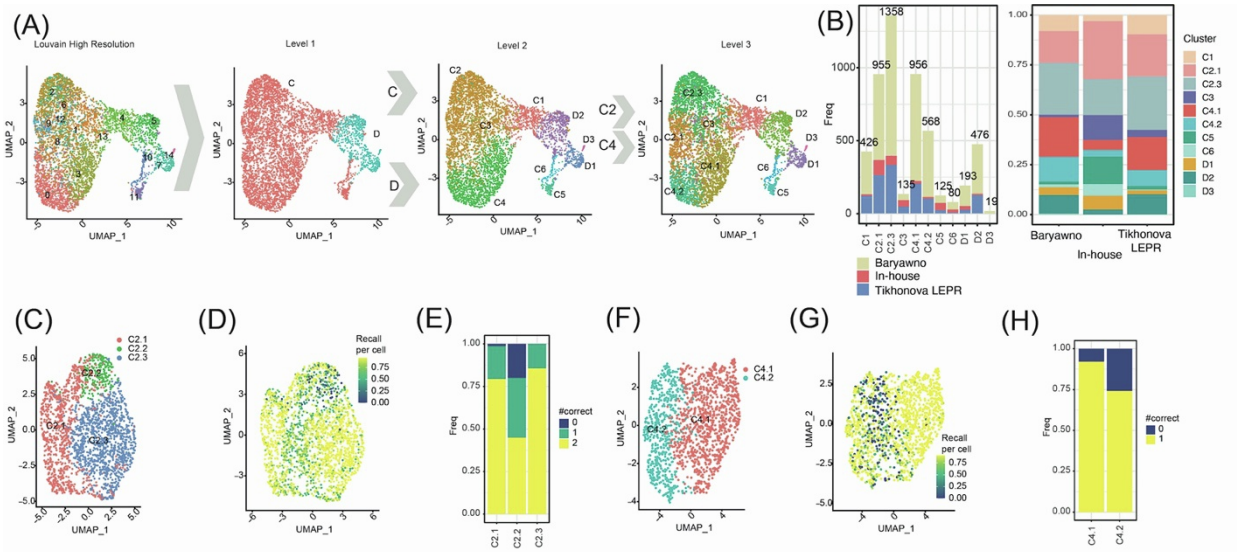

Figure S3. High-resolution clustering strategy of mesenchymal cells, related to Figure 2.
(A) Clustering strategy: Mesenchymal. An upper limit to cluster is set for the clustering (left panel) using Louvain high-resolution clustering. Then, an iterative divide-and-conquer strategy identifies the optimal level of clusters for a given set of cells, and, within each cluster, it evaluates possible sub-clustering. Level 1 (second panel from the left), Level 2 (third panel) and Level 3 (fourth panel) shows the clustering after every iteration. **(B)** Left: representation of the number of cells for each cluster and contribution of each data set to final mesenchymal clusters. Right: proportions of subclusters in each data-set. **(C-E)** Robustness of the analysis for sub-clustering C2 (from Level 2 to Level 3). Specifically: **(C)** Illustration of the identified clusters**; (D)** Depiction of every cell, *how many times it is assigned correctly to a cluster using a random-forest + bootstrapping strategy* (see Methods); **(E)** Summary of the results (d) per cluster. **(F-H)** Demonstration of the same analysis for cluster C4.

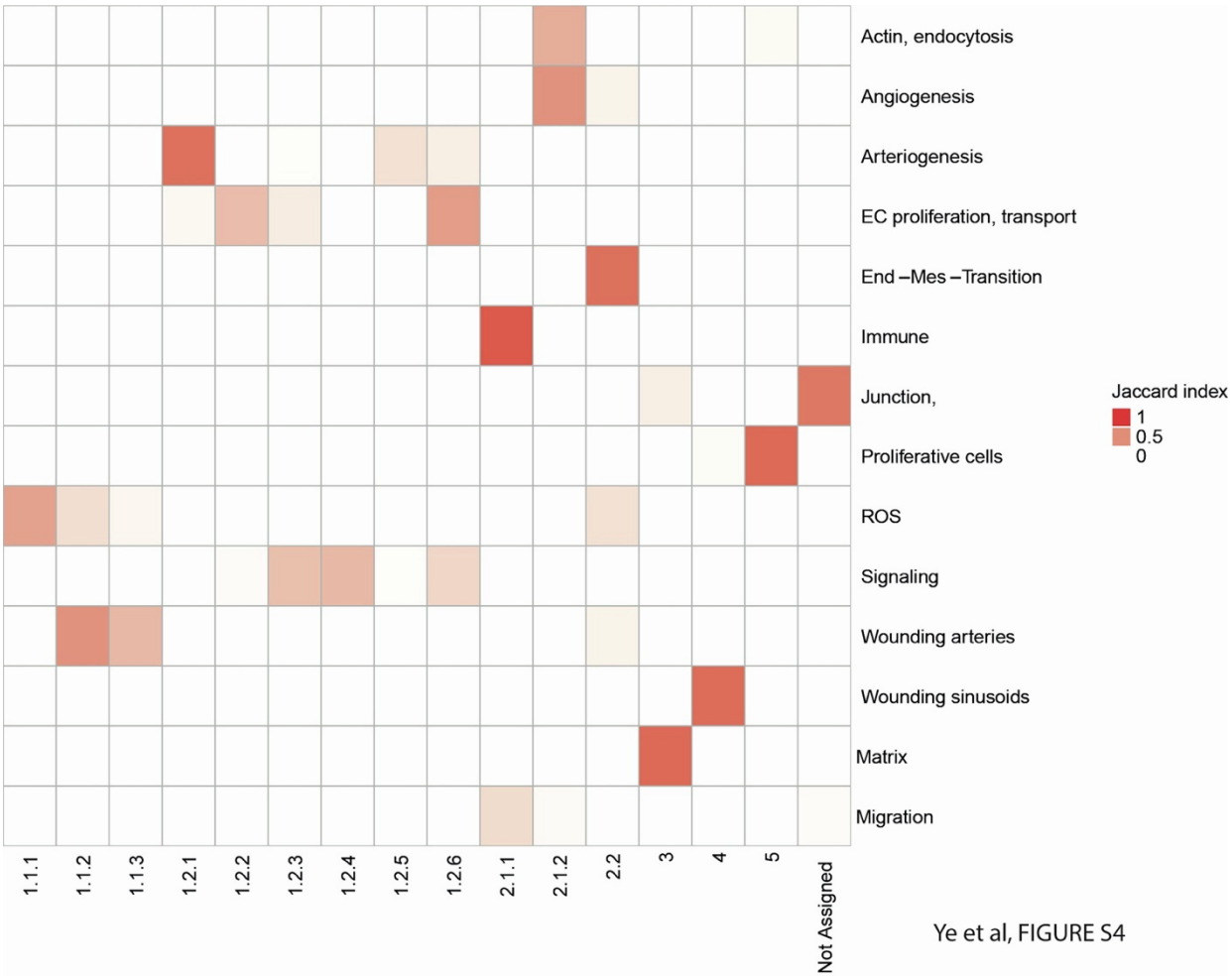

Figure S4. Added value: identification of clusters, related to Figure 3, 4 and 5. Pairwise Jaccard Index analysis between Baryawno dataset only and the identified clusters observed with the integrated dataset (rows).

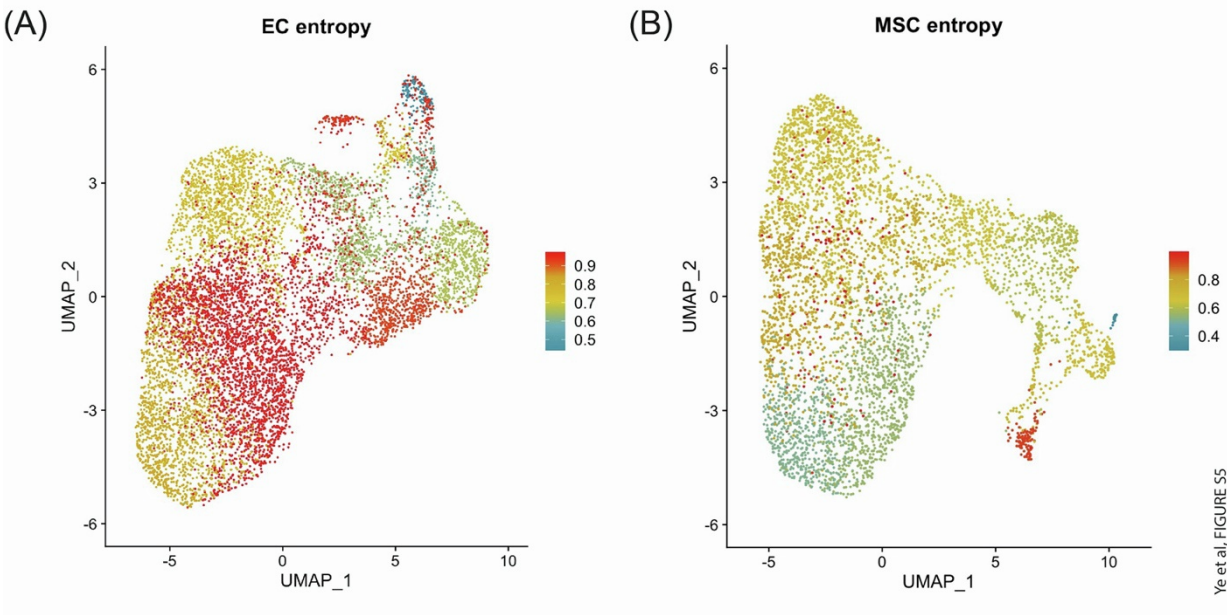

Figure S5. Entropy Analysis, related to Figure 3. **(A)** Entropy analysis of EC cells. **(B)** Entropy analysis of MSC cells.

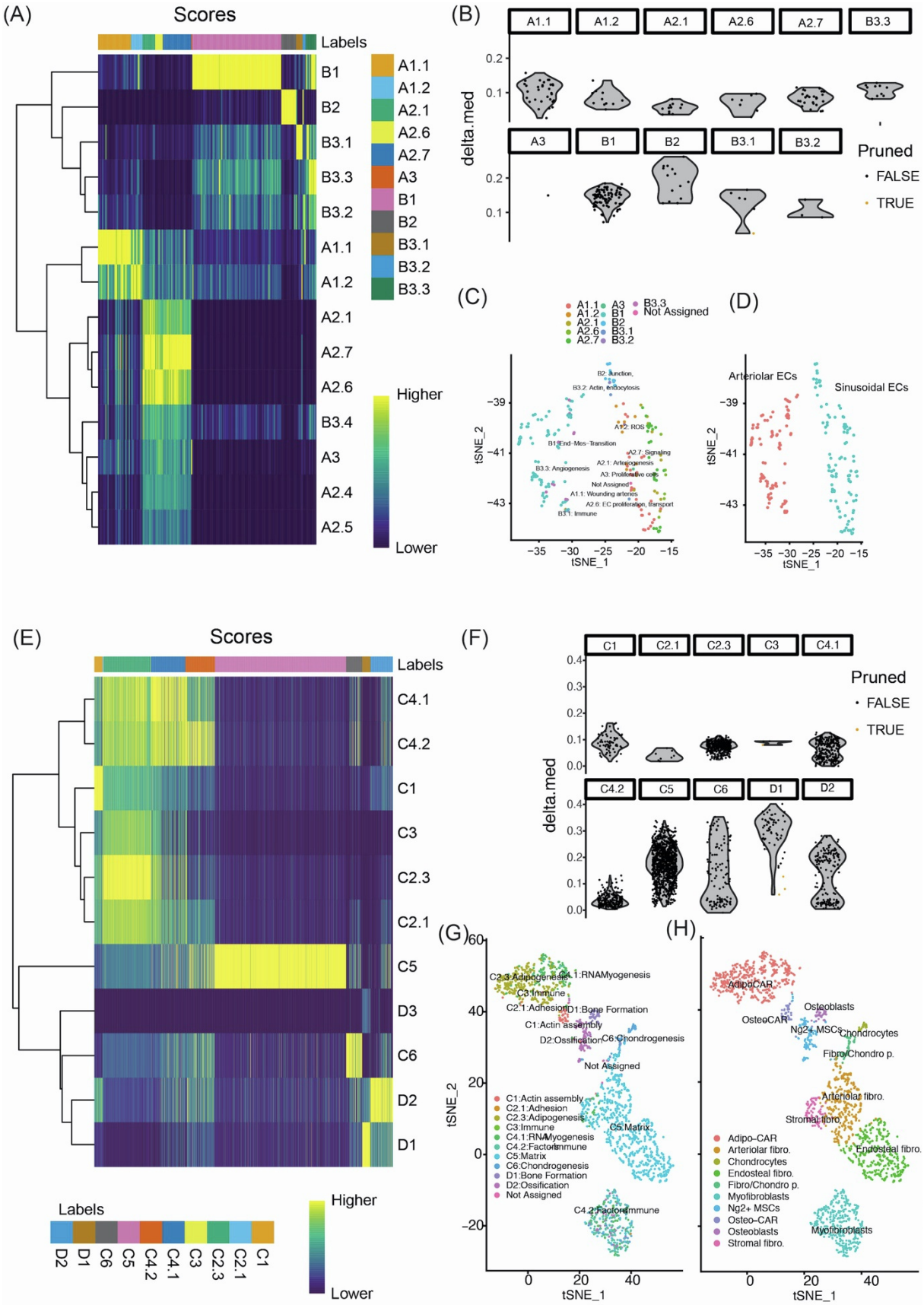

Figure S6. Annotation of Baccin et al, cells. related to Figure 7. **(A)** Heatmap score-derived with the annotations and scores assigned to EC cells. **(B)** EC Score distribution per cluster after cells assigned to clusters based on score. **(C)** t-SNE plot of EC Baccin et al. data-set with assigned annotations. **(D)** t-SNE plot of EC Baccin et al. data-set with original annotations. **(E,F,G,H)** are similar to (A,B,C,D) respectively but considering MSC analysis.

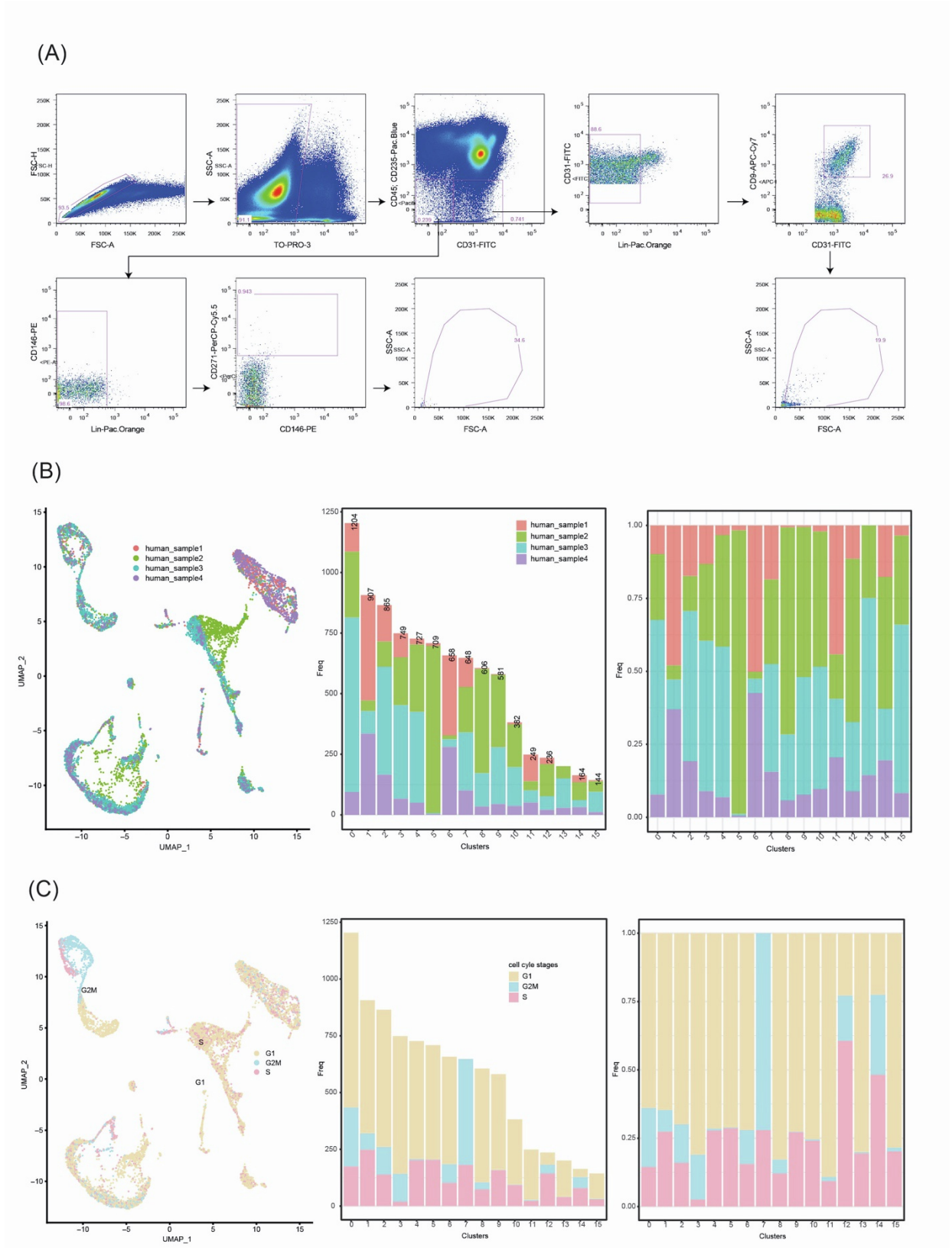

Figure S7. Analysis of human samples, related to Figure 6 **(A)** Cell sorting strategy for isolation of human bone marrow endothelial (TO-PRO-3^{-}, Lin^{-}, CD45^{-}, CD235^{-}, CD9^{+}, CD31^{+}) and mesenchymal-osteolineage (TO-PRO-3^{-}, Lin^{-}, CD45^{-}, CD235^{-}, CD31^{-}, CD271^{+}, CD146$^{+/-}$) cells. **(B)** Left panel: UMAP representation of cells quantified after filtering showing the sample of origin; Middle Panel: number of cells per cluster and sample of origin; Right panel: proportion of cells per cluster and sample of origin. **(C)** Left panel: UMAP visualization of cells quantified after filtering and showing the cell cycle stage; Middle Panel: number of cells per cluster and cell cycle stage; Right panel: proportion of cells per cluster and cell cycle stage.

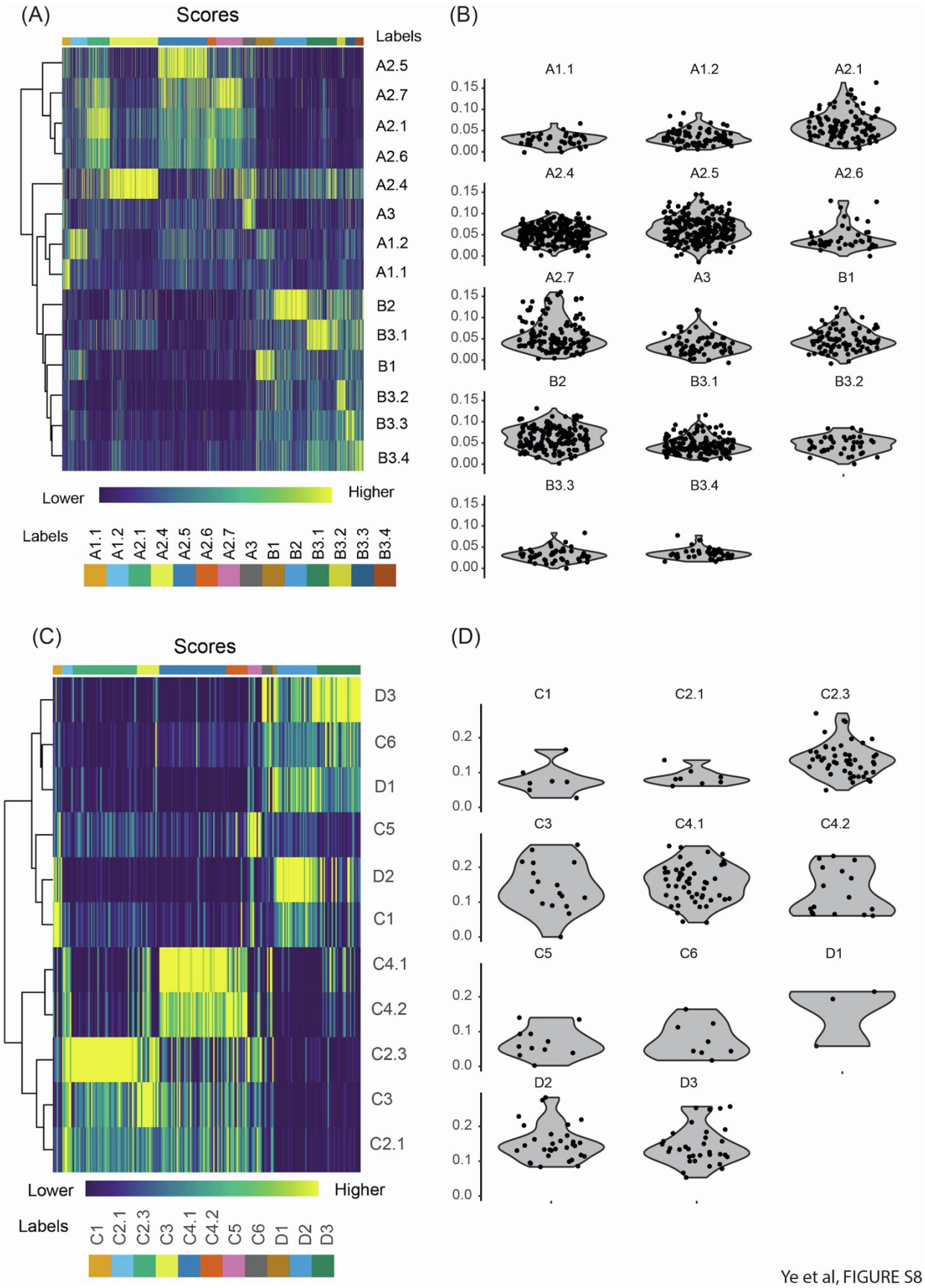

Ye et al, FIGURE S8

Figure S8. Conservation analysis of the EC and MSC population in the human BM microenvironment, related to Figure 7. Annotation of the human cells using the identified endothelial (**A**) and mesenchymal (**C**) mouse markers through SingleR analysis. Violin plots of the associated scores for endothelial (**B**) and mesenchymal (**D**) subclusters.

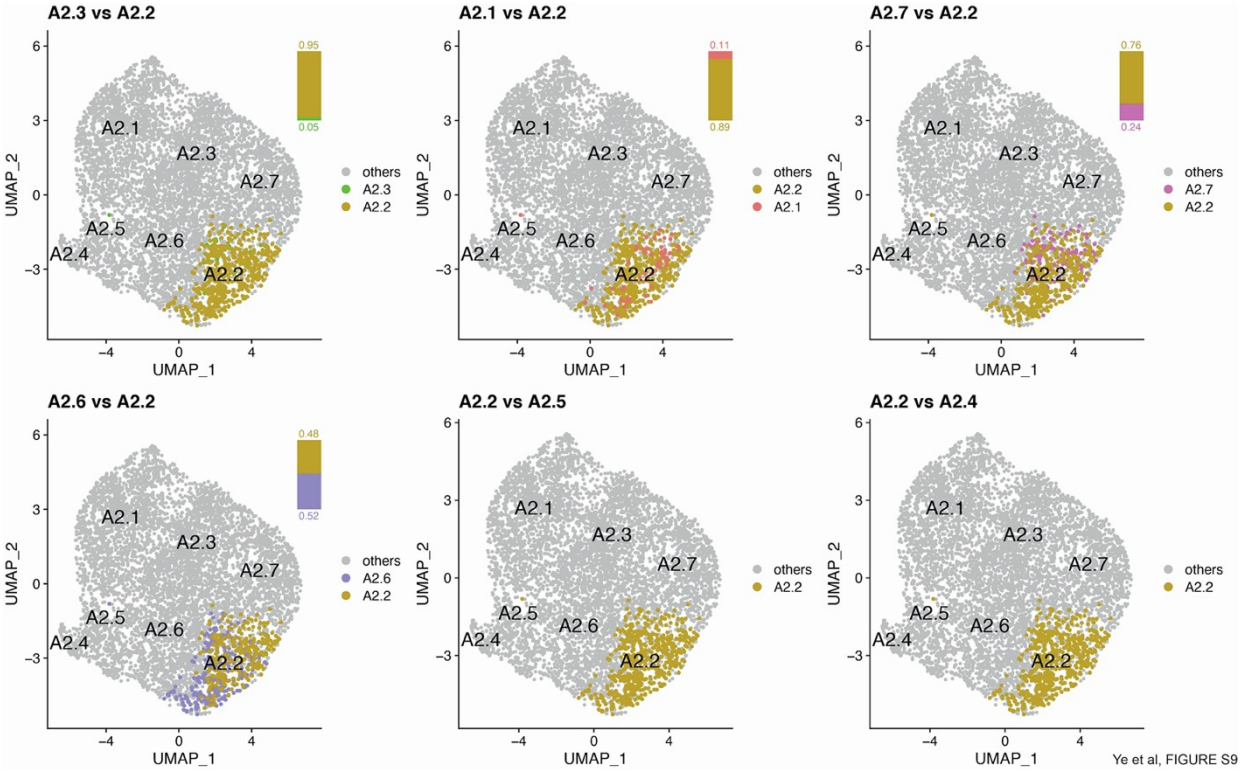

Figure S9. Assignment of cells from non-robust clusters, related to STAR Methods. Example of how cells can be assigned to other clusters once they have been identified as non-robust.